Published in final edited form as:
J Psychiatr Res. 2012 August ; 46(8): 1045–1052. doi:10.1016/j.jpsychires.2012.04.013.

Functional MRI of the amygdala and bed nucleus of the stria terminalis during conditions of uncertainty in generalized anxiety disorder

Michael A. Yassa[1,*], **Richard L. Hazlett**[2], **Craig E. L. Stark**[3], and **Rudolf Hoehn-Saric**[2,*]

[1]Department of Psychological and Brain Sciences, Johns Hopkins University, Baltimore, MD

[2]Department of Psychiatry and Behavioral Sciences, Johns Hopkins School of Medicine, Baltimore, MD

[3]Department of Neurobiology and Behavior, Center for Neurobiology of Learning and Memory, University of California at Irvine, Irvine, CA

Abstract

Generalized anxiety disorder (GAD) is a common psychiatric disorder characterized by constant worry or anxiety over every day life activities and events. The neurobiology of the disorder is thought to involve a wide cortical and subcortical network that includes but is not limited to the amygdala and the bed nucleus of the stria terminalis (BNST). These two regions have been hypothesized to play different roles in stress and anxiety; the amygdala is thought to regulate responses to brief emotional stimuli while the BNST is thought to be involved in more chronic regulation of sustained anxiety. In this study, we exposed medication-free GAD patients as well as non-anxious controls to a gambling game where one of the conditions involved non-contingent monetary loss. This condition of high uncertainty was intended to elicit a stressful response and sustained anxiety. Functional MRI scans were collected simultaneously to investigate BOLD activity in the amygdala and BNST during performance of this task. Compared to controls, we found that GAD patients demonstrated *decreased* activity in the amygdala and *increased* activity in the BNST. Skin conductance measures showed a consistent early versus late effect within block where GAD patients demonstrated higher arousal than controls late in the task blocks. Based on these results, we hypothesize that GAD patients disengage the amygdala and its response to acute stress earlier than non-anxious controls making way for the BNST to maintain a more sustained response. Future studies are needed to investigate the temporal dynamics of activation and deactivation in these regions.

Introduction

Generalized anxiety disorder is characterized by chronic worry, possibly due to abnormalities in regulating emotional processing (Mennin et al., 2005; McLaughlin et al.,

Additional author contact information: Richard Hazlett, Ph.D., 2045 York Road, 3rd Floor, Baltimore, MD 21093. Craig E. L. Stark, Ph.D., 211 Qureshey Research Lab, UC Irvine, Irvine, CA 92697. . [*]**Corresponding Authors: Michael A. Yassa, Ph.D.***(will handle correspondence with the journal)* Psychological and Brain Sciences 3400 N. Charles St., Ames 216A Baltimore MD 21218-2686 Tel: (410) 516-0202, Fax: (410) 516-4478 yassa@jhu.edu; **Rudolf Hoehn-Saric, M.D.** Psychiatry and Behavioral Sciences 600 N. Wolfe St., Meyer 4-109 Baltimore MD 21287-7409 Tel: (410) 439-9671, Fax: (410) 955-0946 rhoehn@jhmi.edu.

2007). This regulation involves a wide network of brain regions, which encompasses the extended amygdala (including the bed nucleus of the stria terminalis, BNST) and the prefrontal cortex. The role of the amygdala in processing emotional stimuli is relatively well established in animal (Davis, 2006) and human studies (Kent & Rauch, 2004; Costafreda et al., 2008; Sergerie et al., 2008). However, its role in modulating fear and anxiety in generalized anxiety disorder (GAD) is less well understood.

Although one might predict that GAD involves a heightened amygdala response to fearful or anxiety-provoking stimuli (Etkin & Wager, 2007), studies in GAD patients have often provided conflicting results. Several studies have noted greater amygdala activation to noxious stimuli in pediatric and adolescent GAD samples (McClure et al., 2007; Monk et al., 2008). However, studies in adults have been less consistent. Some have reported in GAD patients a heightened amygdala response to all stimuli, including non-aversive ones, (Hoehn-Saric et al., 2004a; Nitschke et al., 2009), while others have found no group differences in levels of amygdala fMRI BOLD activation between GAD patients and controls during processing of emotional stimuli (Whalen et al., 2008; Etkin et al., 2010). One study also reported a *reduced* amygdala response to fearful faces in GAD patients (Blair et al., 2008).

Davis and colleagues (Davis, 1998; Walker et al., 2003; Davis, 2006; Walker & Davis, 2008; Walker et al., 2009; Davis et al., 2010) have suggested that fear and anxiety may be expressed through two separate but complementary systems, a rapid response system that mediates short-term responses to threatening stimuli and includes the central nucleus of the amygdala (phasic fear) and a second system that includes the BNST, which while sluggish in response, continues to influence behavior long after the initiating stimulus has been terminated (sustained fear or “anxiety”).

The BNST is a region of the extended amygdala complex that consists of a heterogeneous group of nuclei (Walker & Davis, 2008). The pattern of connectivity in the BNST suggests that this region acts as a relay center coordinating the activity of autonomic, neuroendocrine, and somatic motor systems into fully organized physiological functions and behavior (Dumont, 2009), possibly under the control of the medial prefrontal cortex (Spencer et al., 2005). The BNST may also receive emotional and learning-associated information and possibly plays a role in integrating these inputs with reward/motivational circuits (Jalabert et al., 2009). The BNST is thought to maintain sustained anxiety-like responses in animals (Walker et al., 2003), such as the gradual elevation in baseline startle seen in animals over the course of training (Gewirtz et al., 1998). Stress-induced “hyperanxiety” in rats is correlated with increased volumes of the BNST but not the amygdala; this appears to be driven by dendritic remodeling in anteromedial areas, which are implicated in emotional and neuroendocrine control of stress responses (Pego et al., 2008). Thus, the BNST appears to be highly plastic and is in a key position to regulate stress and anxiety responses.

The role of the BNST in anxiety disorders has not been systematically examined, with two notable exceptions. A human fMRI study of spider phobics (Straube et al., 2007), found that the anticipation of adverse visual stimuli activated the BNST but not the amygdala. Another study of healthy participants with varying degrees of trait anxiety (Somerville et al., 2010) found that during observation of a fluctuating line, which provided information relevant to subsequent risk of electric shocks, participants showed increased activity in the BNST but not in the amygdala. This response was pronounced in more anxious individuals. Thus, sustained anxiety led to an increased engagement of the BNST but not the amygdala.

In this study, we used a non-contingent monetary loss task which involves high uncertainty on a trial-by-trial basis to attempt to induce a state of sustained anxiety while we explored

the nature of BOLD fMRI responses in the amygdala and the BNST in individuals with and without GAD. Based on previous work by Straube et al. (2007) and Somerville et al. (2010) as well as the Davis model discussed above, we predicted that we would find a potentiated BNST response in GAD patients compared to controls and that there would be no group differences in amygdala activity. Consistent with our first prediction, we observed enhanced activity in the BNST in GAD patients in the "high-uncertainty" condition. Somewhat surprisingly, however, we found *decreased* amygdala activation in GAD patients in the same condition. This suggests that these two brain regions might be operating in different and possibly opposite ways, supporting observations from animal studies.

Materials and Methods

Participants

Fifteen right-handed medication-free patients diagnosed with GAD according to DSM-IV criteria and no other pathology and fifteen right-handed controls underwent a psychiatric and medical examination that included the Structured Clinical Interview for DSM-IV (SCID-IV) and a urine toxicology screen. See Table 1 for clinical and demographic data. Participants were recruited on the Johns Hopkins medical campus through advertisement, screened by telephone and subsequently evaluated by a psychiatrist (R.H-S.). Signed informed consent was obtained from all participants prior to the study. Participants received $100 for their participation. Diagnosed patients also received a free one hour counseling session and, when necessary, a referral for further treatment.

Neuropsychological evaluation

In addition to psychiatric evaluation and clinical diagnosis, each study participant was administered the Hamilton Anxiety Inventory (HAM-A: Hamilton, 1959), the Hamilton Depression Scale (HAM-D: Hamilton, 1960), the State-Trait Anxiety Scale, Trait Form (STAI-T: Spielberger et al., 1970), and the Somatic Symptoms Scale (SSS: Hoehn-Saric et al., 1989). Scores on these scales are summarized in Table 1 with statistical comparisons of group means. We also collected self-ratings data from all participants after the scan to determine if the task successfully raised anxiety levels. Self-ratings questionnaires instructed participants to rate the following variables on a Likert scale from 1-10 with 10 being the highest score possible: pleasant/happy, anxious/worried, irritable/angry, and sad/disappointed. Each participant provided a rating in each of these categories for the control task (color judgment) and another rating for the monetary task.

Behavioral and self-report statistical analysis

Behavioral data (accuracy and reaction time) were analyzed using two-way repeated measures ANOVAs with group as a between-subject variable and condition as a within-subject variable. Self-report data were analyzed using several two-way ANOVAs (one for each dependent measure) with group as a between-subject variable and condition as a within-subject factor. All statistical analyses were conducted in R v. 2.14.1 (R Foundation for Statistical Computing, www.R-project.org).

fMRI paradigm

We used non-contingent monetary loss to increase the level of uncertainty in participants. The task consisted of three conditions: Low-uncertainty, high-uncertainty, and control. During the low-uncertainty condition, participants had the opportunity to quickly develop a strategy and maintain monetary gain. During the high-uncertainty condition, probabilities of monetary gain were altered such that participants had difficulty developing a successful strategy and almost always lost money. In both of these conditions, two colored squares

appeared on the screen, one on top of the other (Figure 1). Participants were instructed to guess which of the two squares on the screen will lead to monetary gain (plus $1) and not loss (minus $2). Participants were given immediate post-trial feedback. During the low-uncertainty blocks, the blue square had a 100% probability of winning money, whereas the yellow square only had a 50% probability of winning money. Thus, participants quickly learned to select the correct square leading to consistent monetary gain. During the high-uncertainty blocks both squares only had a 50% probability of winning money. Thus, participants were unable to establish an effective strategy and almost always lost money.

During the control blocks, red and green-colored squares appeared on the screen. Participants were instructed to press the button corresponding to the location of the red square. In the control condition, there was no monetary gain or loss involved and no post-trial feedback was given. If participants had a net positive balance at the end of the task, they were paid that additional amount as a bonus for their performance. If they had a negative balance, they were only paid for their participation. The task consisted of 4 blocks (12 trials each) of each active condition and 8 control blocks (20 trials each). The task was developed in MATLAB 7.0 (The Mathworks, Sherborn, MA) using Cogent 2000 (Functional Imaging Laboratory, Wellcome Department of Imaging Neuroscience, University College, London, UK).

Image acquisition

Images were acquired on a Philips 3-Tesla MRI scanner (Philips Medical Systems, Eindhoven, The Netherlands) equipped with an 8-channel SENSitivity Encoding (SENSE) head coil, located at the F.M. Kirby Research Center for Functional Brain Imaging at the Kennedy Krieger Institute (Baltimore, MD). Functional T2*-weighted images were acquired using an echoplanar single shot pulse sequence with the following parameters (matrix size = 80 × 80, TE = 30 ms, flip angle = 75°, TR = 1500 ms, resolution = 3.2 mm × 3.2 mm × 3 mm + 1 mm inter-slice gap, 30 slices parallel to AC-PC). A high-resolution (1 mm isotropic) 3D MP-RAGE sequence was also acquired for anatomical localization (FOV = 256, matrix = 256 × 256, 150 axial slices). We used several procedures to correct for fMRI signal distortions. First, we employed higher-order shims, which can directly compensate for local field distortions. Second, by using SENSE parallel imaging which utilizes multiple surface coils to undersample k-space with fewer phase encoding steps, we significantly reduced our acquisition time. This limited distortion resulting from magnetic susceptibility.

Imaging data processing and analysis

Functional image preprocessing and analysis was performed using Analysis of Functional NeuroImages (AFNI) software (Cox, 1996). Time periods in which a significant motion event (more than 3 degrees of rotation or 2 mm of translation in any direction) occurred plus and minus one TR were censored and subsequently eliminated from the analysis. A box-car function convolved with a canonical hemodynamic response function was used to model the data using a general linear model (GLM). A regressor was specified for each of the two active conditions (high-uncertainty and low-uncertainty), with the control condition acting as a baseline. Two contrasts were constructed: a comparison of high vs. low uncertainty, and an active (high + low uncertainty) vs. control comparison.

In order to gain maximum sensitivity to subtle changes in fMRI signal in the BNST and the amygdala, we used a regional high-dimensional cross-participant alignment approach (described in detail in the next section). The aligned data was subsequently smoothed with a modest 4 mm FWHM smoothing kernel to minimize global individual variability and improve the fit of the data to statistical assumptions.

Region-of-Interest Segmentation and Cross-Participant Alignment

Cross-participant brain alignment began with a standard whole-brain alignment. Each participant's functional scans underwent a 6-parameter rigid transformation (3 rotations and 3 translations in X, Y, and Z directions) followed by a 12-parameter piecewise linear transformation to Talairach space (Talairach & Tournoux, 1988). This was then fine-tuned using a region-of-interest alignment approach (Stark & Okado, 2003; Miller et al., 2005; Kirwan et al., 2007; Yassa & Stark, 2009; Yassa et al., 2010b). We manually segmented the amygdala, the hippocampus, and the caudate on every participant's MPRAGE scan. Regions of interest were isolated using reliable published protocols for the hippocampus and medial temporal cortices (Insausti et al., 1998), amygdala (Honeycutt et al., 1998), and caudate (Aylward et al., 1996).

The hippocampus was first segmented by starting in the most lateral slice where it was visible in the sagittal plane and proceeding in the medial direction until it completely disappeared. The superior boundary was set by the amygdala rostrally and the choroid fissure and the lateral ventricle caudally. The white matter of the parahippocampal gyrus served as the inferior boundary. The amygdala was then segmented on axial slices using the uncus and temporal horn of the lateral ventricle as the posterior boundary in superior slices and using the hippocampus itself as the posterior boundary in inferior slices. The lateral boundary was defined by an arbitrary line drawn from the most medial white matter to the lateral fissure excluding gray matter medial to this line. The medial boundary was set by the hippocampal uncus in anterior slices and by white matter in the posterior slices. The inferior boundary was set by surrounding white matter. Finally, the caudate was segmented also in the axial view using the internal capsule as the medial boundary and the lateral ventricle as the lateral boundary.

The goal from segmenting these structures was to surround the BNST with high accuracy cross-participant alignment using known and easily identifiable regions, thereby significantly improving the cross-participant alignment of the BNST itself. The cross-participant alignment of these segmentations was done using Region of Interest Large Deformation Diffeomorphic Metric Mapping (ROI-LDDMM: Miller et al., 2005). This method smoothly transformed each participant's regions of interest into the same space as a 3D template segmentation, while critically preserving regional boundaries and the integrity of the space between these boundaries. First, we used this alignment to create a "modal model" of the segmentations based on the entire sample. We then calculated the deformation fields required to morph each participant's scan into this common space. This transformation was then applied to each participant's fMRI statistical map, increasing the sensitivity of group comparisons. We have demonstrated in the past that this technique yields superior alignment and detection power on fMRI scans in the regions of interest (Miller et al., 2005; Yassa & Stark, 2009).

Once the scans were averaged across participants, we also manually outlined the BNST and amygdala on the average structural scan in order to restrict our ROI analyses to those regions (the BNST is visible on this higher SNR average scan). For the amygdala we used the same protocol previously used for individual participants (Honeycutt et al., 1998). We drew a boundary around the BNST region according to expert anatomical knowledge provided by the late Dr. Lennart Heimer (Heimer, L. *personal communication*). The BNST was first located in the coronal view at the crossing (midline) of the anterior commissure where it is prominently located as a triangular area between the internal capsule, the anterior commissure and the lateral ventricle. Its rostral extension was estimated until it finally disappeared ~3mm rostral to the crossing of the anterior commissure. The caudal extension was estimated until the anterior commissure disappeared into the temporal lobe.

Clustering and Statistical Analysis

Patient and control groups were compared using a two-way ANOVA to investigate any differences in stress-related activity across groups and across conditions. Group (GAD, control) and condition (high-uncertainty, low-uncertainty, and control) were both entered as fixed factors, with subject treated as a random factor nested within group. A peak threshold of $P < 0.05$ on the overall F statistic was combined with a spatial extent threshold of 10 voxels to identify task-related voxels and filter out task-irrelevant voxels. This approach, rather than using a direct pair-wise contrast, reduces voxel selection biases (Baker et al., 2007). The thresholded statistical maps were then combined with the anatomical segmentations for the amygdala and BNST to only include voxels inside those ROIs, creating hybrid functional/anatomical ROIs. We have used this method successfully in the past for regional analyses of the medial temporal lobes (Yassa et al., 2010a; Yassa et al., 2010b; Lacy et al., 2011; Yassa et al., 2011). Voxels within each hybrid anatomical/functional ROI were then collapsed for further analysis. Mean collapsed ROI signals were compared across groups using *post hoc* contrasts.

Skin Conductance Measurement

Skin conductance data was collected during the fMRI scans with standard silver/silver chloride electrodes attached to the palm of the non-dominant hand. A PsyLab SCR-SA skin conductance module (Contact Precision Instruments) provided a constant voltage across electrodes. The signal was sent through shielded cables to an analog/digital converter that digitized the signal at a rate of 50 Hz. Skin conductance during the low-uncertainty, high-uncertainty, and control conditions was calculated by taking the median value during each block. For each condition, the median values for each participant were averaged across blocks and runs to yield the three scores. One GAD patient was missing Run 1 data, and this participant was excluded from the analyses. For temporal analyses of SCR data, we normalized the raw conductance data and then used repeated measures ANOVA to compare groups and conditions.

Results

Behavioral results

Average accuracy and latency values are shown in Table 2. We used a repeated measures ANOVA with group as a between-subject variable and condition as a within-subject variable. For accuracy, we found a significant main effect of condition ($F_{1,28} = 346.7$, $P < .05$) but no significant effect of group ($F_{1,28} = .05$, $P > .05$) nor a group by condition interaction ($F_{1,28} = 1.39$, $P > .05$). For latency, we found similar results; a significant main effect of condition ($F_{1,28} = 4.95$, $P < .05$) but not for group ($F_{1,28} = .26$, $P > .05$) or group by condition interaction ($F_{1,28} = .78$, $P > .05$). These results suggest that performance was lower on the high uncertainty condition compared to the low uncertainty condition, both in terms of accuracy and reaction time. However, there were no significant differences on either measure between groups.

Self-report measures

Average responses for the self-report measures are shown in Table 3. We used a repeated measures ANOVA with group as a between-subject variable and condition as a within-subject variable for each of the dependent measures. Mauchley's Test of Sphericity was not significant for condition, thus no correction for error nonsphericity was conducted. We found a significant main effect of group ($F_{1,28} = 10.26$, $P < .05$) as well as a significant main effect of condition ($F_{1,28} = 19.43$, $P < .05$) in rating the task as "pleasant/happy". The interaction was not significant ($F_{1,28}$ .083, $P > .05$). This suggests that "Pleasant/happy"

ratings were higher across both groups for the control condition vs. the active condition and were also higher in the control group vs. the GAD group across active and control conditions. The opposite pattern was found for "anxious/worried" ratings where the ratings were higher in the GAD group across conditions and higher in the active condition across groups. Here, we found a significant main effect of group ($F_{1,28}$ = 5.35, P < .05) as well as a significant main effect of condition ($F_{1,28}$ = 21.20, P < .05). The interaction was also not significant ($F_{1,28}$ = .32, P > .05). The same pattern was found for the "irritated/angry" ratings. We found a significant main effect of condition ($F_{1,28}$ = 41.42, P < .05) and a marginally significant main effect of group ($F_{1,28}$ = 2.60, P = .12). The interaction once again was not significant ($F_{1,28}$ = .16, P > .05). Finally, "sad/disappointed" ratings showed a slightly different picture where we found a significant main effect of condition ($F_{1,28}$ = 44.21, P < .05) but no significant main effect of group ($F_{1,28}$ = .23, P > .05), nor a group × condition interaction ($F_{1,28}$ = .65, P > .05). It appears that across both groups, all individuals tended to rate the active condition as "sad/disappointing" much more than the control condition. Overall, the self-rating data indicate that the monetary task was associated with higher self-reported anxiety and irritability across groups, and that this effect was exaggerated in the GAD group.

fMRI results

Both groups activated the amygdala and BNST bilaterally during the contrast of the active conditions (high + low uncertainty) compared to the control condition. However, we found no statistically significant group differences on this contrast. We observed group differences in the contrast of high-uncertainty (50% probability condition) to the low-uncertainty (100% probability condition). Here, we found a statistically significant group difference in the bilateral amygdala (t_{28}=-2.14, P < .05; Cohen's d = −.81) and a difference approaching significance in the bilateral BNST (t_{28}=1.66, P = .1). The pattern of difference in those two regions were exactly opposite of one another. We found *increased* activation in the bilateral BNST and *decreased* activation in the bilateral amygdala in patients compared to controls (see Figure 2).

Skin conductance results

Elevations in anxiety and stress were computed by comparing the median values of skin conductance during the high and low uncertainty conditions with the skin conductance medians during the control conditions. The mean for the control condition was 3.81 microsiemens (st. error = 0.48) across all participants and 3.96 microsiemens for the active conditions (st. error = 0.5). Using a repeated measures ANOVA, we found a significant main effect in comparing the active conditions (high + low uncertainty) to the control condition ($F_{1,27}$ = 22.79, P < .001). There was not a main effect of group (GAD vs. controls) ($F_{1,27}$ = 1.66, P > .05), nor interaction between condition and group ($F_{1,27}$ = .95, P > .05).

We next plotted the z-transformed skin conductance responses on a second-by-second analysis to investigate the potential role of temporal effects (Figure 4A). We split the data into three 20-second temporal bins to compare early (1-20 seconds), middle (21-40 seconds), and late (41-60 seconds) phases of the block (Figure 4B). We conducted a repeated measures ANOVA with group as a between subject variable and both condition (active vs. baseline) and temporal bin (early vs. middle vs. late) as within-subject variables. Mauchley's Test of Sphericity was significant for both temporal bin and the interaction of condition*temporal bin, thus reported degrees of freedom for these variables are Greenhouse Geisser (GG) corrected for error nonsphericity. We found no significant main effect of either condition ($F_{1,28}$ = .28, P > .05) or group ($F_{1,28}$ = .73, P > .05) nor an interaction between condition and group ($F_{1,28}$ = .30, P > .05). We did find a significant main effect of temporal bin ($F_{1.3,36.4(GG)}$ = 171.25, P < .05) as well as a significant interaction between

group and temporal bin ($F_{1.3,36.4(GG)} = 4.27$, $P < .05$). Neither the interaction between condition and temporal bin ($F_{1.2,34.2(GG)} = .12$, $P > .05$) nor the three-way interaction between condition, group and temporal bin bin ($F_{1.2,34.2(GG)} = .35$, $P > .05$) was significant. The data suggests that GAD patients start the block with a lower SCR than controls, but unlike controls, their SCR reactivity remains elevated by the end of a 60-second block. This explains the lack of a significant main effect of group despite the significant interaction with temporal bin.

Correlation between skin conductance and fMRI

We observed a significant correlation between the change in skin conductance response (SCR) and the change in BOLD fMRI response in the amygdala in high vs. low uncertainty conditions in the controls group (*Pearson* $r = .51$, $P < .05$; Fig 5B), but not in the GAD group (*Pearson* $r = -.09$, $P > .05$; Fig 5A). To further determine if this difference between group correlations is statistically reliable, we converted the correlations using a Fisher's r-to-z transformation. The correlation between SCR and amygdala activity in the GAD group was $z_r = 0.55$. The correlation in the control group was $z_r = -.098$. The difference between the two z-scores was $z = .65$ ($P = .26$) which was not statistically significant.

Discussion

The present study compared fMRI brain activation patterns in medication-free generalized anxiety disorder patients and healthy controls during a non-contingent monetary loss task intended to use uncertainty to elicit sustained anxiety. Based on animal models of phasic and sustained fear (i.e. anxiety), we predicted that the BNST would be engaged in this task. Further, we predicted that its activity levels would be increased in patients compared to controls. We found evidence for our prediction when comparing the high-uncertainty condition (where participants almost always lost money by not being able to use a successful strategy) to the low-uncertainty condition (where participants easily gained money by always being able to use the same strategy). Previous studies showed that anticipation of a potentially negative event, an unstructured and prolonged adverse condition, was associated with increased activity in the BNST (Straube et al., 2007; Somerville et al., 2010). Our findings are largely consistent with results from these studies and extend the finding of elevated BNST responses to individuals with generalized anxiety disorder.

Interestingly, we also found that the level of amygdala activity was diminished in patients compared to controls during the same contrast. Previous studies have not investigated amygdala activity during prolonged stressful tasks in anxiety patients. Our findings suggest that GAD patients may disengage or even suppress amygdala activity during prolonged anxiety or stress. A recent report by Alvarez and colleagues (2011) found evidence for increased BOLD activity in the BNST during situations where threat was unpredictable, but not in situations where threat was predictable, consistent with animal models of phasic and sustained fear (Davis et al., 2010). The authors noted that the amygdala may be activated transiently at the beginning of a prolonged stressful episode, but eventually gives way to the activation of the BNST complex to maintain anxiety.

Extending the argument from Alvarez and colleagues (2011), we hypothesize that in GAD patients the amygdala might be engaged early in the course of a stressful or threatening event, but quickly disengages to allow the BNST to maintain an a continuous anxious state and that this process may be more exaggerated compared to non-anxious individuals. This would explain why we observed amygdala suppression and BNST enhancement in GAD patients in our task, although given the nature of our blocked design, these temporal relations were difficult to assess. We conducted an exploratory analysis based on these observations that modeled activity during task blocks with a monotonically decreasing

function and found a trend ($P < 0.1$) towards higher activity in the amygdala in GAD patients vs. controls in the high vs. low uncertainty contrast, suggesting that GAD patients may indeed be disengaging the amygdala earlier than controls. However, due to the exploratory nature of this analysis, the below-significant results, as well as the fact that our design did not lend itself to addressing these temporal relationships, we will not comment further on this finding except to say that this is an important future direction of investigation.

One additionally interesting question that we could not address in our study is whether network interactions are different in GAD patients and controls. In order to investigate this further, one would need to perform resting fMRI scans to examine anxiety-related differences in functional connectivity between the amygdala and the BNST, another important question for future studies.

The results of the current study are interpreted in terms of responses to varying levels of uncertainty, however this is not the only possible cognitive factor involved. Other potential differences related to top-down control mechanisms could also contribute to the results observed. These factors include processing load, working memory capacity, increased attention, and response conflict. It is likely, however, that these factors would induce differences outside of the network of regions of interest in the study. The amygdala and BNST are part of a larger cortical network and cognitive control mechanisms may play a significant role in the interaction between the BNST and the amygdala (Hoehn-Saric et al., 2005; McClure et al., 2007; Monk et al., 2008). For example, cognitive activity (Hariri et al., 2003) or worry (Hoehn-Saric et al., 2005; Schienle et al., 2009) attenuates amygdala activity while deliberately focusing on one's anxiety enhances the response (McClure et al., 2007). The effects of cognitive activity on BNST activity are not well studied but can provide interesting clues as to the dynamics of this larger network.

On average, skin conductance was higher across all participants in the active conditions compared to the baseline condition, although there was no significant difference between the two active conditions nor an interaction with patient status. This suggests that in general, the task was effective at raising anxiety levels, although this may have been similar across conditions and participant groups. A more detailed analysis of temporal patterns within blocks revealed an interesting effect of time. We noted a robust effect of temporal bin (early vs. middle vs. late) on skin conductivity and an interaction with group such that GAD patients started task blocks with a lower conductivity than controls, but ended the blocks with a higher conductivity than controls. This suggests that GAD patients had a diminished ability to reduce arousal throughout the task block, which is expected given the psychiatric phenotype and prior literature. This response pattern, namely an initially weak but subsequently prolonged physiological response to stimuli, which we called diminished physiological flexibility, has been previously demonstrated in patients with GAD and with other anxiety disorders (Hoehn-Saric et al., 2004b).

We also found a positive correlation between levels of amygdala activation and skin conductance response in controls only and not in GAD patients. This can be partly explained by the observation that amygdala levels of activity are suppressed in GAD patients while skin conductance levels remain elevated in this group beyond controls. This could presumably lead to a decoupling between cognitive and physiological variables, which may otherwise be coupled in healthy adults. Previous research has also indicated that correlations between physiological responses and subjective somatic perceptions were present in controls but not in GAD patients (Hoehn-Saric et al., 2004b), consistent with the idea that there is a decoupling of cognitive and physiological variables in GAD patients. It is important to note, however, that a direct comparison of the correlations between the two groups was not

statistically reliable, suggesting that this difference is marginal at best and should not be interpreted too strongly.

A notable strength of this study was the use of a superior segmentation and cross-participant registration technique that enabled us to conduct this regional investigation. The BNST is a small structure that is very difficult to identify on MRI scans. Even small amounts of registration error could result in completely missing activity changes in this region. We maximized our sensitivity by segmenting regions around the BNST (striatum and limbic lobe) to enhance the overlap in the BNST in our group analyses. We have shown before that this method results in increased detection power in functional maps (Miller et al., 2005; Kirwan et al., 2007; Yassa & Stark, 2009).

The study had several limitations that should be noted. First, the sample sizes used were quite small (15 in each group), perhaps underpowered to detect additional group differences that did not survive statistical threshold. Thus, replicating these results with a larger sample will be important. Second, our blocked design did not allow us to directly assess temporal relationships including within-block habituation in the amygdala. Future studies using mixed block and event-related designs will be important in answering these questions. Third, the task used was intended to be a direct manipulation of stress levels using uncertainty. It appears that both the high and low uncertainty conditions increased physiological arousal but not to a differential degree. Future studies using behavioral and psychophysical designs that allow for parametric manipulations of stress and anxiety levels should be conducted.

We conclude that generalized anxiety disorder is associated with enhanced BNST responses and diminished amygdala responses during conditions of uncertainty that elicit stress/anxiety, potentially signaling key changes in network dynamics that should be the subject of further examination.

References

Alvarez RP, Chen G, Bodurka J, Kaplan R, Grillon C. Phasic and sustained fear in humans elicits distinct patterns of brain activity. Neuroimage. 2011; 55:389–400. [PubMed: 21111828]

Aylward EH, Codori AM, Barta PE, Pearlson GD, Harris GJ, Brandt J. Basal ganglia volume and proximity to onset in presymptomatic Huntington disease. Arch Neurol. 1996; 53:1293–1296. [PubMed: 8970459]

Baker CI, Hutchison TL, Kanwisher N. Does the fusiform face area contain subregions highly selective for nonfaces? Nat Neurosci. 2007; 10:3–4. [PubMed: 17189940]

Blair K, Shaywitz J, Smith BW, Rhodes R, Geraci M, Jones M, McCaffrey D, Vythilingam M, Finger E, Mondillo K, Jacobs M, Charney DS, Blair RJ, Drevets WC, Pine DS. Response to emotional expressions in generalized social phobia and generalized anxiety disorder: evidence for separate disorders. Am J Psychiatry. 2008; 165:1193–1202. [PubMed: 18483136]

Costafreda SG, Brammer MJ, David AS, Fu CH. Predictors of amygdala activation during the processing of emotional stimuli: a meta-analysis of 385 PET and fMRI studies. Brain Res Rev. 2008; 58:57–70. [PubMed: 18076995]

Cox RW. AFNI: software for analysis and visualization of functional magnetic resonance neuroimages. Comput Biomed Res. 1996; 29:162–173. [PubMed: 8812068]

Davis M. Are different parts of the extended amygdala involved in fear versus anxiety? Biol Psychiatry. 1998; 44:1239–1247. [PubMed: 9861467]

Davis M. Neural systems involved in fear and anxiety measured with fear-potentiated startle. Am Psychol. 2006; 61:741–756. [PubMed: 17115806]

Davis M, Walker DL, Miles L, Grillon C. Phasic vs sustained fear in rats and humans: role of the extended amygdala in fear vs anxiety. Neuropsychopharmacology. 2010; 35:105–135. [PubMed: 19693004]

Dumont EC. What is the bed nucleus of the stria terminalis? Prog Neuropsychopharmacol Biol Psychiatry. 2009; 33:1289–1290. [PubMed: 19602427]

Etkin A, Prater KE, Hoeft F, Menon V, Schatzberg AF. Failure of anterior cingulate activation and connectivity with the amygdala during implicit regulation of emotional processing in generalized anxiety disorder. Am J Psychiatry. 2010; 167:545–554. [PubMed: 20123913]

Etkin A, Wager TD. Functional neuroimaging of anxiety: a meta-analysis of emotional processing in PTSD, social anxiety disorder, and specific phobia. Am J Psychiatry. 2007; 164:1476–1488. [PubMed: 17898336]

Gewirtz JC, McNish KA, Davis M. Lesions of the bed nucleus of the stria terminalis block sensitization of the acoustic startle reflex produced by repeated stress, but not fear-potentiated startle. Prog Neuropsychopharmacol Biol Psychiatry. 1998; 22:625–648. [PubMed: 9682277]

Hamilton M. The assessment of anxiety states by rating. Br J Med Psychol. 1959; 32:50–55. [PubMed: 13638508]

Hamilton M. A rating scale for depression. Journal of Neurology, Neurosurgery, and Psychiatry. 1960; 23:56–62.

Hariri AR, Mattay VS, Tessitore A, Fera F, Weinberger DR. Neocortical modulation of the amygdala response to fearful stimuli. Biol Psychiatry. 2003; 53:494–501. [PubMed: 12644354]

Hoehn-Saric R, Lee JS, McLeod DR, Wong DF. Effect of worry on regional cerebral blood flow in nonanxious subjects. Psychiatry Res. 2005; 140:259–269. [PubMed: 16297605]

Hoehn-Saric R, McLeod DR, Zimmerli WD. Somatic manifestations in women with generalized anxiety disorder. Psychophysiological responses to psychological stress. Arch Gen Psychiatry. 1989; 46:1113–1119. [PubMed: 2589925]

Hoehn-Saric, R.; McLeod, DR. Somatic manifestations of normal and pathological anxiety. In: Hoehn-Saric, R.; McLeod, DR., editors. Biology of Anxiety Disorders. American Psychiatric Press; Washington DC: 1993. p. 177-223.

Hoehn-Saric R, Schlund MW, Wong SHY. Effects of citalopram on worry and brain activation in patients with generalized anxiety disorder. Psychiatry Research: Neuroimaging. 2004a; 131:11–21.

Hoehn-Saric R, McLeod DR, Funderburk F, Kowalski P. Somatic symptoms and physiologic responses in general anxiety and panic disorder: an ambulatory monitor study. Archives of General Psychiatry. 2004b; 61:913–921. [PubMed: 15351770]

Honeycutt NA, Smith PD, Aylward E, Li Q, Chan M, Barta PE, Pearlson GD. Mesial temporal lobe measurements on magnetic resonance imaging scans. Psychiatry Res. 1998; 83:85–94. [PubMed: 9818734]

Insausti R, Juottonen K, Soininen H, Insausti AM, Partanen K, Vainio P, Laakso MP, Pitkanen A. MR volumetric analysis of the human entorhinal, perirhinal, and temporopolar cortices. AJNR Am J Neuroradiol. 1998; 19:659–671. [PubMed: 9576651]

Jalabert M, Aston-Jones G, Herzog E, Manzoni O, Georges F. Role of the bed nucleus of the stria terminalis in the control of ventral tegmental area dopamine neurons. Prog Neuropsychopharmacol Biol Psychiatry. 2009; 33:1336–1346. [PubMed: 19616054]

Kent, JM.; Rauch, SL. Neuroimaging studies of anxiety disorders. In: Charney, DS.; Nestler, EJ., editors. Neurobiology of Mental Illnesses. 2nd ed. Oxford University Press; New York: 2004. p. 639-660.

Kirwan CB, Jones CK, Miller MI, Stark CE. High-resolution fMRI investigation of the medial temporal lobe. Hum Brain Mapp. 2007; 28:959–966. [PubMed: 17133381]

Lacy JW, Yassa MA, Stark SM, Muftuler LT, Stark CE. Distinct pattern separation related transfer functions in human CA3/dentate and CA1 revealed using high-resolution fMRI and variable mnemonic similarity. Learn Mem. 2011; 18:15–18. [PubMed: 21164173]

McClure EB, Monk CS, Nelson EE, Parrish JM, Adler A, Blair RJ, Fromm S, Charney DS, Leibenluft E, Ernst M, Pine DS. Abnormal attention modulation of fear circuit function in pediatric generalized anxiety disorder. Arch Gen Psychiatry. 2007; 64:97–106. [PubMed: 17199059]

McLaughlin KA, Mennin DS, Farach FJ. The contributory role of worry in emotion generation and dysregulation in generalized anxiety disorder. Behav Res Ther. 2007; 45:1735–1752. [PubMed: 17270145]

Mennin DS, Heimberg RG, Turk CL, Fresco DM. Preliminary evidence for an emotion dysregulation model of generalized anxiety disorder. Behav Res Ther. 2005; 43:1281–1310. [PubMed: 16086981]

Miller MI, Beg MF, Ceritoglu C, Stark C. Increasing the power of functional maps of the medial temporal lobe by using large deformation diffeomorphic metric mapping. Proc Natl Acad Sci U S A. 2005; 102:9685–9690. [PubMed: 15980148]

Monk CS, Telzer EH, Mogg K, Bradley BP, Mai X, Louro HM, Chen G, McClure-Tone EB, Ernst M, Pine DS. Amygdala and ventrolateral prefrontal cortex activation to masked angry faces in children and adolescents with generalized anxiety disorder. Arch Gen Psychiatry. 2008; 65:568–576. [PubMed: 18458208]

Nitschke JB, Sarinopoulos I, Oathes DJ, Johnstone T, Whalen PJ, Davidson RJ, Kalin NH. Anticipatory activation in the amygdala and anterior cingulate in generalized anxiety disorder and prediction of treatment response. Am J Psychiatry. 2009; 166:302–310. [PubMed: 19122007]

Pego JM, Morgado P, Pinto LG, Cerqueira JJ, Almeida OF, Sousa N. Dissociation of the morphological correlates of stress-induced anxiety and fear. Eur J Neurosci. 2008; 27:1503–1516. [PubMed: 18336570]

Schienle A, Schafer A, Pignanelli R, Vaitl D. Worry tendencies predict brain activation during aversive imagery. Neurosci Lett. 2009; 461:289–292. [PubMed: 19545612]

Sergerie K, Chochol C, Armony JL. The role of the amygdala in emotional processing: a quantitative meta-analysis of functional neuroimaging studies. Neurosci Biobehav Rev. 2008; 32:811–830. [PubMed: 18316124]

Somerville LH, Whalen PJ, Kelley WM. Human bed nucleus of the stria terminalis indexes hypervigilant threat monitoring. Biol Psychiatry. 2010; 68:416–424. [PubMed: 20497902]

Spencer SJ, Buller KM, Day TA. Medial prefrontal cortex control of the paraventricular hypothalamic nucleus response to psychological stress: possible role of the bed nucleus of the stria terminalis. J Comp Neurol. 2005; 481:363–376. [PubMed: 15593338]

Spielberger, CD.; Gorsuch, RL.; Lushene, RE. Manual for the State-Trait Anxiety Inventory. Consulting Psychologists Press; Palo Alto CA: 1970.

Stark CE, Okado Y. Making memories without trying: medial temporal lobe activity associated with incidental memory formation during recognition. J Neurosci. 2003; 23:6748–6753. [PubMed: 12890767]

Straube T, Mentzel HJ, Miltner WH. Waiting for spiders: brain activation during anticipatory anxiety in spider phobics. Neuroimage. 2007; 37:1427–1436. [PubMed: 17681799]

Talairach, J.; Tournoux, P. Co-planar stereotaxic atlas of the human brain: 3-dimensional proportional system: an approach to cerebral imaging. Thieme Medical; New York: 1988.

Walker DL, Davis M. Role of the extended amygdala in short-duration versus sustained fear: a tribute to Dr. Lennart Heimer. Brain Struct Funct. 2008; 213:29–42. [PubMed: 18528706]

Walker DL, Miles LA, Davis M. Selective participation of the bed nucleus of the stria terminalis and CRF in sustained anxiety-like versus phasic fear-like responses. Prog Neuropsychopharmacol Biol Psychiatry. 2009; 33:1291–1308. [PubMed: 19595731]

Walker DL, Toufexis DJ, Davis M. Role of the bed nucleus of the stria terminalis versus the amygdala in fear, stress, and anxiety. Eur J Pharmacol. 2003; 463:199–216. [PubMed: 12600711]

Whalen PJ, Johnstone T, Somerville LH, Nitschke JB, Polis S, Alexander AL, Davidson RJ, Kalin NH. A functional magnetic resonance imaging predictor of treatment response to venlafaxine in generalized anxiety disorder. Biol Psychiatry. 2008; 63:858–863. [PubMed: 17964548]

Yassa MA, Lacy JW, Stark SM, Albert MS, Gallagher M, Stark CE. Pattern separation deficits associated with increased hippocampal CA3 and dentate gyrus activity in nondemented older adults. Hippocampus. 2010a; 21:968–979. [PubMed: 20865732]

Yassa MA, Mattfeld AT, Stark SM, Stark CE. Age-related memory deficits linked to circuit-specific disruptions in the hippocampus. Proc Natl Acad Sci U S A. 2011; 108(21):8873–8. [PubMed: 21555581]

Yassa MA, Stark CE. A quantitative evaluation of cross-participant registration techniques for MRI studies of the medial temporal lobe. Neuroimage. 2009; 44:319–327. [PubMed: 18929669]

Yassa MA, Stark SM, Bakker A, Albert MS, Gallagher M, Stark CE. High-resolution structural and functional MRI of hippocampal CA3 and dentate gyrus in patients with amnestic Mild Cognitive Impairment. Neuroimage. 2010b; 51:1242–1252. [PubMed: 20338246]

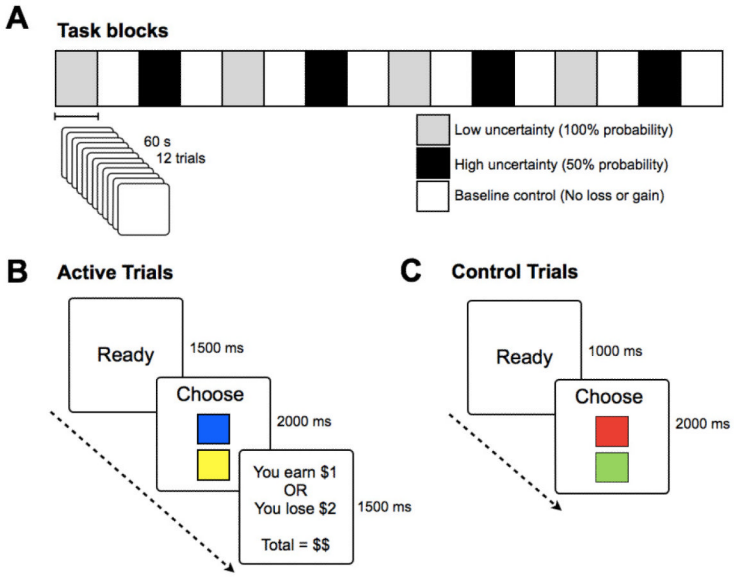

Figure 1.

(A) Task blocks and timing parameters for each run. (B) Trial sequence for stress trials ("ready" screen, followed by "choice" screen, followed by feedback, and (C) Trial sequence for control trials ("ready" screen, followed by "choice" screen and no feedback is given).

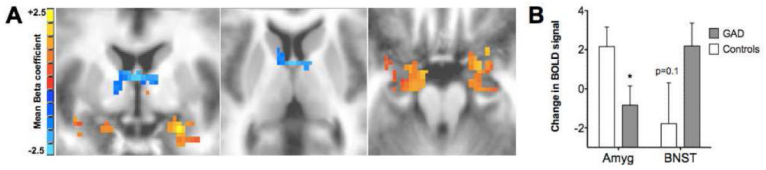

Figure 2.

(A) Group contrast of Controls minus GAD patients shown at an uncorrected *P* value of .05 with a 10-voxel cluster threshold. *Increases* in activity in controls compared to GAD patients are shown in red (bilateral amygdala) while *decreases* are shown in blue (bilateral BNST). These maps are not restricted to the anatomical ROIs and thus some additional activity overlapping with the hippocampus and the caudate is also shown. Only activity inside our anatomical ROIs entered the statistical analysis. Representative coronal and axial slices are depicted. (B) Statistical comparison of bilateral amygdala and BNST activity in GAD patients and controls showing decreased amygdala activity and increased BNST activity in patients.

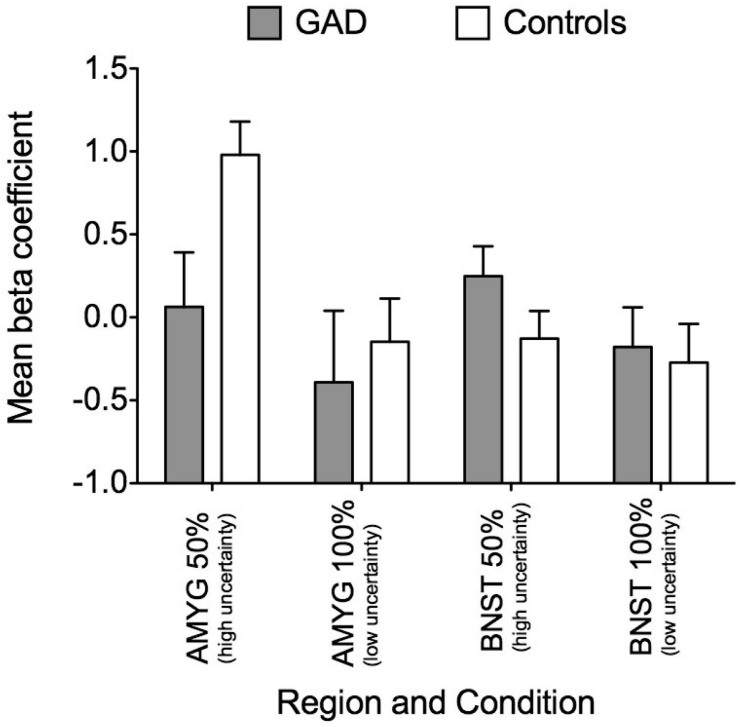

Figure 3.
Comparison of group × ROI activity across active task conditions.

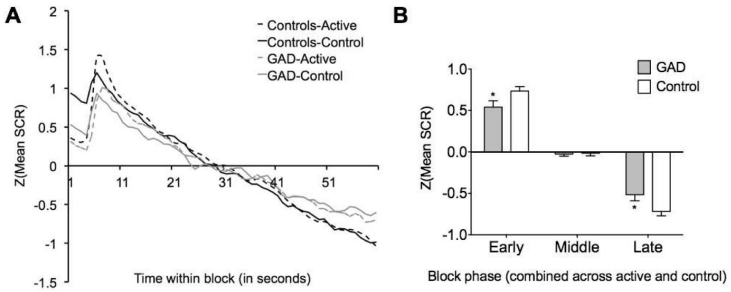

Figure 4.

Analysis of skin conductance within-block temporal effects. (A) a second-by-second depiction of group × task condition conductance showing a possible group difference that could have been obscured by the time-averaged analysis, (B) A more quantitative evaluation of early vs. middle vs. late temporal effects and comparison across groups, demonstrating clear evidence of decreased conductance at the beginning of the block and increased conductance at the end of the block in GAD patients compared to controls.

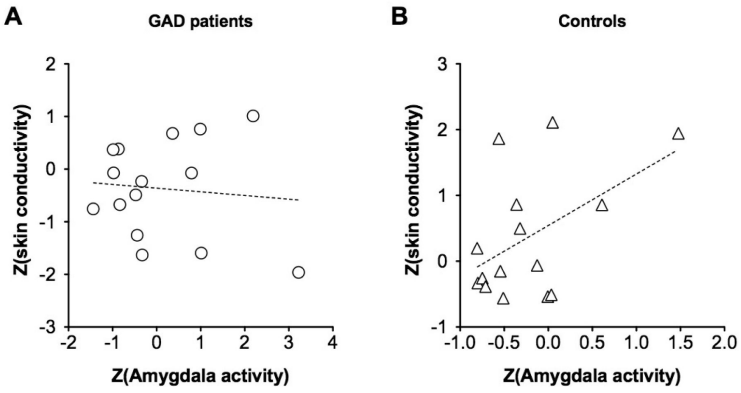

Figure 5.
Correlations between z-transformed skin conductance response in the uncertainty conditions and the z-transformed fMRI BOLD response in the amygdala. There is a significant correlation between amygdala activation and SCR response in controls (B) but not in GAD patients (A).

Table 1

Participant Demographics and Neuropsychological Evaluation

	GAD patients	Controls	*P*-value
N	15	15	
Age	34.7 (9.5)	32.5 (8.7)	ns
Gender	12F: 3M	9F: 6M	ns[e]
Years of education	17.1 (2.1)	17.0 (2.6)	ns
HAM-A [a]	23.1 (3.7)	1.6 (1.8)	<.001
STAI-T [b]	50.6 (7.5)	27.4 (5.2)	<.001
SSS [c]	18.1 (9.0)	1.4 (1.2)	<.001
HAM-D [d]	7.3 (2.2)	0.8 (0.39)	<.001

Data reported as mean (standard deviation)

[a] Hamilton Anxiety Inventory

[b] State-Trait Anxiety Scale, Trait form

[c] Somatic Symptoms Scale

[d] Hamilton Depression Scale

[e] Tested using Fischer's exact test (all others tests used unpaired t-test)

Table 2

Behavioral Data

Group	Low Uncertainty		High Uncertainty	
	Accuracy	Latency	Accuracy	Latency
GAD Patients	81(3)	660 (41)	44 (2)	713 (42)
Controls	84 (1)	645 (31)	42 (2)	768 (43)

Data reported as mean (*standard error of the mean*). Accuracy is reported as a percentage. Latency is in milliseconds.

Table 3

Self-Report Ratings

	GAD patients		Controls	
	Active	**Control**	**Active**	**Control**
Pleasant/Happy	2.5 (0.6)	5.4 (0.9)	4.5 (0.7)	7.8 (0.6)
Worried/Anxious	6.1 (0.7)	3.9 (0.7)	4.7 (0.7)	1.9 (0.4)
Irritated/Angry	6.6 (0.7)	3.1 (0.8)	5.6 (0.8)	1.6 (0.3)
Sad/Disappointed	5.5 (0.6)	1.5 (0.3)	4.8 (0.7)	1.7 (0.4)

Values are reported as mean (*standard error of the mean*)